Research Article

Experimental Study on Reasonable Horizontal Load Value on the Top of Railings of Glass Bridges or Gallery Roads in Scenic Area

Qingwen Sun ⓘ,[1] Qiushi Yan ⓘ,[2] Liqu Liu ⓘ,[3] and Haowei Wang[3]

[1]*China Academy of Building Research, State Key Laboratory of Building Safety and Environment, Beijing 100013, China*
[2]*Key Laboratory of Urban Security and Disaster Engineering, Ministry of Education, Beijing University of Technology, Beijing 100024, China*
[3]*National Center for Quality Supervision and Test of Building Engineering, Beijing 100013, China*

Correspondence should be addressed to Qiushi Yan; yqs2011@bjut.edu.cn

With the increase of glass bridges or glass walkways in the scenic area, the safety protection provided by railings cannot be neglected. However, there is a difference between the demands for a horizontal load on the top of railings in the present design specifications. Especially, it does not give specific advice on the horizontal load on the top of railings of glass bridges or glass roads in the scenic area. In this study, experimental research is conducted on railing columns based on the investigation of common railings of glass bridges or glass roads in the scenic area. The type of railing columns includes finished products and field production. The number of railing columns is 12. The displacement and strain results of the railing columns under different loads are obtained. The rigidity and strength are analyzed by numerical simulation combined with test results. A reasonable horizontal load on the top of the railings of a glass bridge or glass road is advised. These results provide a reference for the design, inspection, and evaluation of railings of glass bridges or gallery roads in the scenic area.

1. Introduction

On March 2, 2021, in a public university in El Alto, Bolivia, the corridor railings suddenly broke, causing seven students to fall and one student to be seriously injured. In the Lantern Festival, in 2004, a crush and stampede accident occurred on the Rainbow Bridge in Mihong Park in Miyun District, Beijing, resulting in 37 deaths and 15 injuries [1]. There have also been many accidents with casualties on campus and shopping malls being caused by collapsed railings [2–4]. At present, glass bridge and gallery road railing systems in scenic areas are designed and manufactured according to the standards of railing systems of civil buildings. Tourists will stop to enjoy and take photos in the steep and dangerous places. Thus, the safety protection of the railing cannot be neglected. It is important to ensure the reliability of railings.

In the existing literature [5–9], different railing systems are verified to satisfy the requirements by the loading test. Fan et al. [10] test the horizontal thrust and vertical pressure of a bridge railing. According to the analysis of the finite element method, the most disadvantageous loading control position of the railing is determined by the design uniform load which is equivalent to the test concentrated load. Zhang and Guo [11] studied the long rail at a bus station by the overall detection method and the cut-off test method. And, the horizontal load of 2.5 kN/m was advised for the railing with two people above. In the existing literature, the study of the horizontal load of railings has not been found.

The load of railings is specifically advised in the present specification. On the top of a railing, the horizontal load value is 1.0 kN/m, and the vertical load value is 1.2 kN/m, according to *Load Code for the Design of Building Structures* (GB 50009-2012) [12]. The horizontal load value is 2.5 kN/m and the vertical load value is 1.2 kN/m e according to *Technical Specifications of Urban Pedestrian Overcrossing and Underpass* (CJJ 69-95) [13]. In addition, according to *Design Specifications for Highway Safety Facilities* (JTG D81-2017) [14], the standard horizontal loading value on the

top of sidewalk or bicycle lane railings is 0.75 kN/m and the standard vertical load value is 1.0 kN/m. According to the uniform building code [15], the load of railings outside the exit is 292 N/m, and the load of railings at the exit is 730 N/m. According to Eurocode [16], both the horizontal load and vertical load are 1.0 kN/m. There is a difference between the horizontal load values in different specifications. Then, the maximum value of the horizontal load is advised in *Technical Specifications of Urban Pedestrian Overcrossing and Underpass* (CJJ 69-95).

For human safety, Hopkins et al. [17] investigated the average pressure of a crowd in a New Year's party and a popular concert in New York, USA. The results showed that people will die in ten minutes in body pressure of 2.1 kN/m and will die in 15 to 30 seconds in a body of 11.68 kN/m. Smith [18] developed an inclined crowd model to quantify the pressure exerted by the crowd on the guard railings. Huang et al. [19] analyzed the pressure bearing capacity of people and individuals by the aforementioned inclined crowd model. The results showed that the safe design load value of human bearing capacity increases from 0.75 to 1.0 kN/m. Therefore, the design value of the horizontal load of railings should be limited.

For railings, structural safety and human safety both should be satisfied. It is necessary to study the reasonable horizontal load value of railings of glass bridges or gallery roads. In this study, experimental research was conducted on railing columns. The type of railing columns includes finished products and field production. The displacement and strain results of the railing columns under different loads are obtained. The rigidity and strength are analyzed by numerical simulation combined with test results. A reasonable horizontal load on the top of the railings of a glass bridge or glass road is advised.

2. Experiment Details

2.1. Simplified Model of Railings. In a railing system, the railing bars are firmly combined with the post which is fixed on the bottom support. The horizontal distributed load F is applied to the railing bars outwards. And, the load is transferred to the post through bar-post joints. The post is the main bearing component. This study focuses on a single post. The horizontal distributed load F of the railing bars is equivalent to concentrated load P applied to the post, as given in equation (1) and Table 1.

The concentrated load:

$$P = F \cdot L, \tag{1}$$

where L is post spacing, calculated as $L = 1$ m.

2.2. Test Methods. There are two types of railing posts for glass bridges or gallery roads in scenic areas based on an investigation. Type I is steel pipe railing posts which are rectangular steel tubes with a thickness of 2 mm–6 mm and a width of 60 mm–120 mm, as shown in Figure 1. Generally, the railing posts and the bottom support are connected by

TABLE 1: Load value.

Load steps	Initial	1	2	3	4	5	6	7	8	9	10	11	12
P (kN)	0	0.5	0.75	1	1.25	1.5	2	2.5	3	3.5	4	4.5	5
F (kN/m)	0	0.5	0.75	1	1.25	1.5	2	2.5	3	3.5	4	4.5	5

FIGURE 1: Example of railings constructed on site.

fillet welds which are 4–6 mm in length. Type II is finished railing posts, assembled on site by the manufacturer, as shown in Figure 2. Type II are single-piece posts made of stainless steel with a thickness of 5 mm–15 mm and a width of 60 mm–120 mm. The bottom gasket of a post is fixed on the bottom support through bolts or welds.

There are two differences between the aforementioned two types of railings. First, the cross sections of the two types of railing posts are different. Second, two types of railing posts are connected to the bottom support in different ways. Finished railings are generally fastened by bolts or spot welding. The steel pipe posts are generally connected by full welding.

Two types of railing posts were tested. Material properties of the selected steel pipe post and the finished post are shown in Table 2 and detailed size parameters are shown in Table 3. The steel pipe post is made of Q235 steel, while the finished post is made of 304 stainless steel. Posts are fixed on the bottom support by welding with 6 mm fillet welds. The nodes at the bottom of the railing posts are fixed with the actual condition consistent. A horizontal loading test was conducted on the top of the post. The displacement, stress, and other test phenomena were recorded. The maximum test load is 5 kN/m.

As shown in Figure 3, the loading system equipment includes a counterforce frame, a load gauge, a displacement sensor, and a strain gauge. The bottom of the post is fixed on the test platform while the top of the post is welded with two railing bars. Displacement measuring points are arranged on the top of the post. Strain measuring points are arranged on its bottom.

2.3. Test Results. The test results of 12 railing posts are summarized in Figure 4. The maximum load, maximum strain, and test phenomena are recorded in Table 4. Posts 1

FIGURE 2: Example of finished railings.

to 8 are steel pipe posts made on site. The steel pipe posts were not collapsed during loading. The maximum load F_{max} applied is 5.0 kN/m. Posts 9 to 12 are finished stainless steel posts. The connections and finished post were damaged due to excessive deformation. The gasket welds at the bottom of the posts were also pulled apart. The maximum load F_{max} applied ranged from 1.5 kN/m to 3.5 kN/m.

At the same displacement, loads of steel pipe posts were compared. As the steel pipe post height increased, both the stiffness of the post and the load value decreased. The load value increased with post section thickness increasing. The load value also increased with post section size increasing. At the same displacement, loads of finished posts were compared. The results showed that the effect of post height, section thickness, and size on the load values of posts can be neglected. The maximum load F_{max} applied for post 1 and 2 was 3.5 kN/m. F_{max} applied for post 3 to 8 was 5.0 kN/m. F_{max} applied for post 9 and 10 was 1.5 kN/m. F_{max} applied for post 11 and 12 was 2.5 kN/m.

The results showed that, for the steel pipe post, the strain under the maximum load was acceptable. For the finished post, the strain increased even under a low load. The load of post 10 was smaller compared with other posts. The possible explanation was that the weld cracking between the post bottom and the gasket lead to a mild increase in the strain of the post.

To sum up, firstly, the effect of post height on the horizontal load value of the steel pipe post is obvious. With the height increase, both the post rigidity and the horizontal load value decreased. Secondly, the maximum test load of the steel pipe post is bigger compared to that of the finished post. At the same load, the strain of the steel pipe post is smaller compared to that of the finished post. Thirdly, the stress of support of the finished post is large with the horizontal load applied.

2.4. Parametric Analysis. Method of normalization was adopted to analyze the test results of steel pipe post 1 to 8 to study the relationship between railing load at the top P, post height H, section property W, material strength f_y, displacement Δ, and strain ε.

(1) The correlation curve of $(FH/W \cdot fy) \propto \Delta/H$ is shown in Figure 5(a). According to *Technical Code*

for Test and Evaluation of City Bridges* (CJJ/T 233-2015) [20], H/120 was taken as the horizontal displacement limit. When $\Delta/H = 1/120$, the value of $(FH/W \cdot fy)$ ranged from 0.15 to 0.31. The correlation curve of $(FH/W \cdot fy) \propto \varepsilon$ is shown in Figure 5(b). When $(FH/W \cdot fy) < 1$, $\varepsilon < 778(\times 10^{-6})$, the maximum strain of components 2, 4, and 7 exceed 500. The maximum strain of other components was less than $400(\times 10^{-6})$. When the value range of $(FH/W \cdot fy)$ ranged from 0.15 to 0.31, the maximum strain is $330(\times 10^{-6})$.

(2) When the displacement limit is $H/120$, the load curve of the steel pipe post is shown in Figure 6. The load value of post 5 was 0.8 kN/m which was the lowest load among posts. The load value of post 8 was 1.9 kN/m which was the highest load. The average load of posts is around 1.2 kN/m.

3. Numerical Analysis

The numerical analysis method was adopted to research more sizes of steel pipe posts in this study. The model of Qi et al. [21] was adopted. In the study of Qi et al. [21], a comparative study was conducted on the between element model and overall model applied on the analysis of the middle part of the column.

The results showed that the results of the internal force and displacement of the middle part column obtained by the element model and overall model are consistent. The element model was proved to analyze the railing system well. The finite element analysis model was developed with *Midas*, as shown in Figure 7(a).

The element model included a post and two half-span railings. One railing is at the left of the post and the other is at the right side. The post bottom was designed to be fixed support. For ends of the railings, the displacement of x, y, and z directions of the node was constrained. Connections between the railing and the post were rigid. The displacement in x, y, and z directions of connections was constrained. The upper node of the post was adopted as the main node. A nodal load was applied on the post based on the element model. And, loading conditions were the same as the test conditions. The material parameters were taken according to the results of material property experiments, as shown in Table 2, and the type of finite element is the bar element. Calculated results are shown in Figures 7(b) and 7(c).

Figure 8 shows the comparison between numerical analysis results and test results.
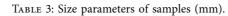
Compared to the results obtained by the experiment, calculated results of deformation and displacement of the railing post using the element model are consistent. Especially, the calculated results' displacement values are the same as the results from the experiment. Therefore, the element model can be used for numerical simulation of the railing posts of glass bridges or gallery roads in the scenic area.

Post height and section size of the post were analyzed. Based on the investigation, most of the steel pipe posts of

TABLE 2: Material properties of samples.

No.	Sample specifications	Elastic modulus E (MPa)	Yield strength f_y (MPa)	Tensile strength (MPa)	Elongation at break (%)
1	Steel pipe post	2.06×10^5	356	503	23.0
2	Finished post	1.93×10^5	700	789	36.5

TABLE 3: Size parameters of samples (mm).

Type	No.	Height	Component size	Thickness
	1	1200	60 * 60	2
	2	1200	60 * 60	3
	3	1200	80 * 80	2
	4	1200	80 * 80	3
Steel pipe post	5	1500	60 * 60	2
	6	1500	60 * 60	3
	7	1500	80 * 80	2
	8	1500	80 * 80	3
	9	1050	60	7
Finished post	10	1050	45–80	14
	11	1000	80	8
	12	1100	60–80	10

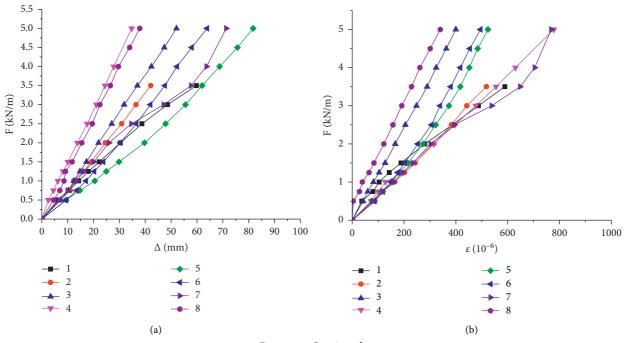FIGURE 3: Schematic diagram of the loading system.
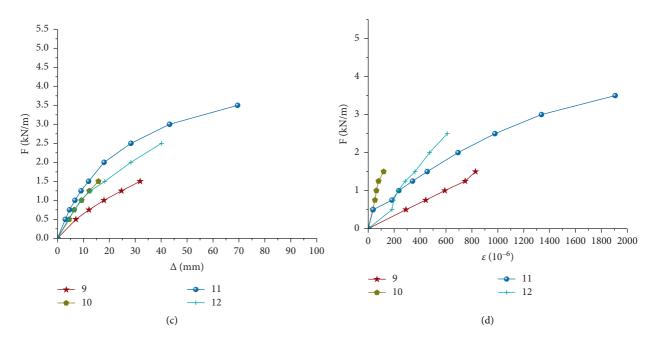

(a)

(b)

FIGURE 4: Continued.

Figure 4: Load-displacement and load-strain test results of post components. (a) Load-displacement test results of steel pipe post components. (b) Load-strain test results of steel pipe post components. (c) Load-displacement test results of finished post components. (d) Load-strain test results of finished post components.

Table 4: Test phenomena.

Type	No.	Maximum load F_{max} (kN/m)	Maximum strain ε (10^{-6})	Description of phenomena
Steel pipe posts	1	3.5	589	The Jack slid out, the test ended; no weld cracked, no post collapsed
	2	3.5	518	The Jack slid out, the test ended, no weld cracked, no post collapsed
	3	5	400	The Jack reached its maximum, the test ended, no weld cracked, no post collapsed
	4	5	778	The Jack reached its maximum, the test ended, no weld cracked, no post collapsed
	5	5	524	The Jack reached its maximum, the test ended, no weld cracked, no post collapsed
	6	5	495	The Jack reached its maximum, the test ended, no weld cracked, no post collapsed
	7	5	768	The Jack reached its maximum, the test ended, no weld cracked, no post collapsed
	8	5	340	The Jack reached its maximum, the test ended, no weld cracked, no post collapsed
Finished posts	9	1.5	828	Welds at the bottom of posts cracked
	10	1.5	119	The upper support broke, the surface of the stainless steel post cracked, and welds between posts and gaskets at the pulling side failed
	11	2.5	1906	The upper support broke, the surface of the stainless steel post cracked
	12	2.5	610	The upper support broke, the surface of the stainless steel post cracked, and welds between posts and gaskets at the pulling side failed

glass bridges and gallery roads in the scenic area were square steel tubes. The height of square steel tubes ranged from 1000 mm to 2000 mm. The section dimension of square steel tubes was (40-100) mm * (2-5) mm. Detailed parameters of the element model are displayed in Table 5. As shown in Table 5, 3 height values and 6 section dimensions of steel pipe posts were adopted, and subsequently, 18 element models were developed for numerical calculation.

The results obtained from 18 element models were analyzed by the method of normalization. The results show that

(1) The relationship of $(FH/W \cdot fy) \propto \Delta/H$ and $(FH/W \cdot fy) \propto \varepsilon$ is shown in Figure 9. The horizontal displacement limit is $H/120$. When $\Delta/H = 1/1201/120$, $(FH/W \cdot fy)$ has a value range
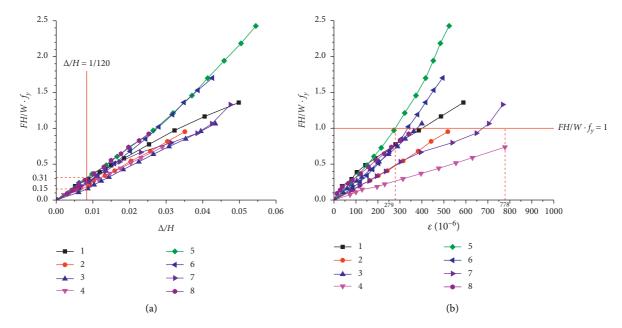
(a)

(b)

FIGURE 5: (a) Correlation curve (test results) of $(FH/W \cdot fy) \propto \Delta/H$. (b) Correlation curve (test results) of $(FH/W \cdot fy) \propto \varepsilon$.
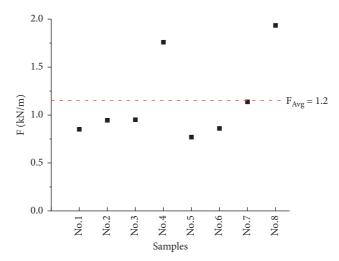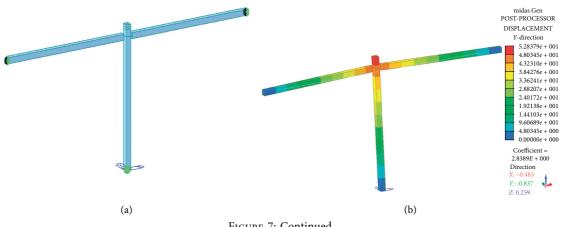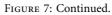

FIGURE 6: Load of steel pipe post with the displacement limit of $H/120$.
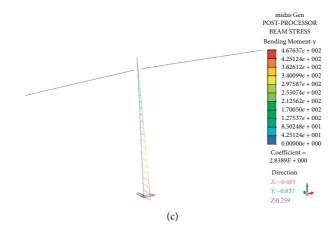

(a)

(b)

FIGURE 7: Continued.

(c)

FIGURE 7: Finite element checking model of railing posts. (a) Element model of a post. (b) Checking results of displacement (post 1). (c) Checking results of stress (post 1).
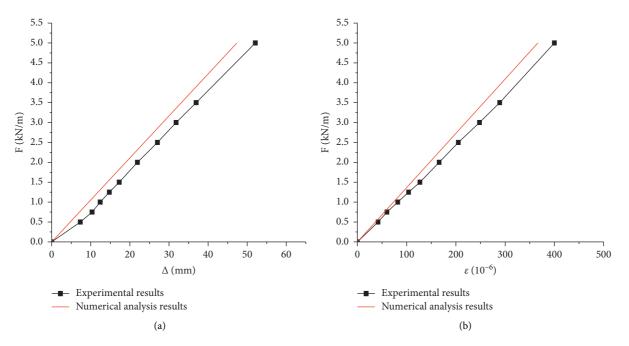

(a)

(b)

FIGURE 8: Comparison of experimental results and numerical analysis results of post 3 ((a) load-displacement; (b) load-strain).

TABLE 5: Size parameters of element models.

	No.	H1	H2	H3	—	—	—
Height	Parameter (mm)	1000	1500	2000	—	—	—
	No.	B1	B2	B3	B4	B5	B6
Section size	Parameter (mm)	50 * 50 * 2	50 * 50 * 5	70 * 70 * 2	70 * 70 * 5	100 * 100 * 2	100 * 100 * 5
	No.	B7	B8	B9	B10	B11	B12
	Parameter (mm)	60 * 60 * 2	60 * 60 * 5	80 * 80 * 2	80 * 80 * 5	90 * 90 * 2	90 * 90 * 5

Note: an element model with a height of 1000 mm and a section size of 50 * 50 * 2 are regarded as H1B1.

from 0.10 to 0.56. The equation ($FH/W \cdot f_y$) can be considered as the ratio between post function S and resistance R. It implied that S/R ranged from 0.10 to 0.56, and equation (2) can be obtained:

When $\dfrac{FH}{W \cdot f_y} < 1 \left(\text{that is } \dfrac{S}{R} < 1 \right), \quad \varepsilon < 230 \left(\times 10^{-6} \right).$

$$(2)$$

(2) When the horizontal displacement limit is $H/120$, the relationship of element model load F and Δ/H is shown in Figure 10. It can be seen that the load of H1B5, H1B6, H2B6, H1B10, and H1B12 were higher than 5.0 kN/m. The load of H3B12 was 0.1 kN/m which was the minimum value. Load values under $\Delta/H = 1/120$ were summarized in Figure 11. The average load was around 1.3 kN/m.
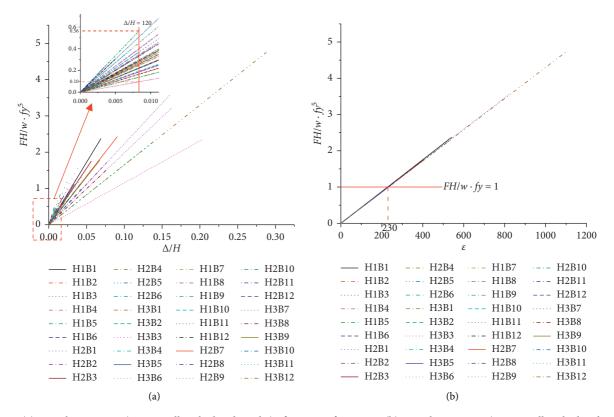
Figure 9: (a) Correlation curve (numerically calculated results) of $FH/W \cdot fy \propto \Delta/H$. (b) Correlation curve (numerically calculated results) of $FH/W \cdot fy \propto \varepsilon$.
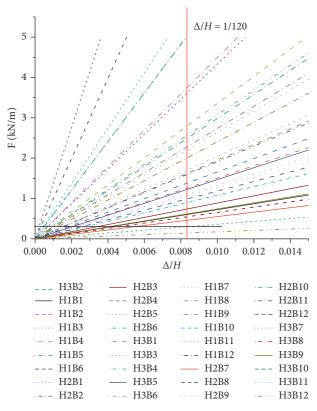

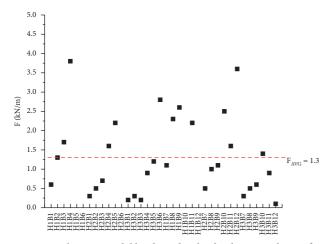Figure 10: Correlation curve of F and Δ/H.

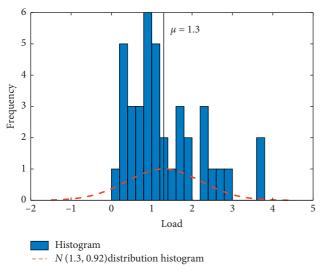FIGURE 11: Element model loads under the displacement limit of $H/120$.

FIGURE 12: Histogram of horizontal load frequencies.

(3) Based on the results of the experiment and simulation, 39 sets of data were used to estimate the averaged horizontal load. The estimated value of averaged horizontal load was 1.3 kN/m. According to results of statistical analysis, the confidence interval of the averaged horizontal load with a confidence level of 95% is given:

$$< \mu >_{0.95} = \left(1.3 - 2.02 \frac{0.92}{\sqrt{39}}; 1.3 + 2.02 \frac{0.92}{\sqrt{39}} \right) \quad (3)$$

$$= (1.0; 1.6) \text{ kN/m}.$$

4. Conclusion

(1) A simplified test model of railings' post was proposed and load tests were carried out on railing posts of different sizes. The results showed that the maximum load of steel pipe posts was 5 kN/m, and the maximum load of finished posts was 2.5 kN/m. Compared with that of finished posts, the maximum load of steel pipe posts was higher and the strain value of steel pipe posts was smaller. Therefore, it is not recommended to choose finished posts as the main stress components in the railing systems of glass bridges and gallery roads in the scenic area.

(2) Results calculated by element models have the same tendency as that of railing posts. Therefore, it is acceptable to use element models for railing post simulation.

(3) Test results of 8 steel pipe posts and 18 steel pipe element models were numerically analyzed. When the displacement limit of the top of the post was $H/120$, $FH/W \cdot fy$ ranged from 0.10 to 0.56, and ε was smaller than $230(\times 10^{-6})$. Therefore, $H/120$ is considered as the displacement limit of the top of the post to ensure that the bearing capacity of the post satisfied the requirements.

(4) With the displacement limit of $H/120$, the average horizontal load of 8 steel pipe posts was 1.2 kN/m and the averaged horizontal load of 18 steel pipe post element models was 1.3 kN/m. Based on analyzing the two sets of data, the confidence interval of the averaged horizontal load with a confidence level of 95% is $< \mu >_{0.95} = (1.0; 1.6)$ kN/m. Therefore, the reasonable value of the horizontal load on the top of the glass bridge or gallery road railings ranged from 1.0 kN/m to 1.6 kN/m.

Data Availability

The data used to support the findings of the study can be obtained upon request (13691371229@163.com).

Conflicts of Interest

The authors declare that they have no conflicts of interest.

References

[1] D. Zhang, "Design of safe evacuation: thoughts on the accident of the rain bowl bridge in Miyun county," *Archicreation*, no. 6, pp. 124–127, 2004.

[2] D. Huang, M. Dong, and Z. Wang, "Analysis and prevention of staircase accidents in primary and secondary schools," *Architectural Technology*, vol. 35, no. 4, pp. 278-279, 2004.

[3] C. Liu, "The Importance of safety design of non-structural building components," *Anhui Architecture*, vol. 11, no. 6, 69 pages, 2004.

[4] J. Liu and W. Xu, "Discussion on firmness and durability of metal railings in civil buildings," *Engineering quality*, vol. 29, no. 8, pp. 5–7, 2011.

[5] L. Chen, "Load test analysis of residential railings," *Shanghai construction technology*, no. 5, pp. 66–70, 2011.

[6] P. Chen, "Horizontal thrust test of pedestrian bridge railing," *Municipal technology*, vol. 29, no. 3, pp. 123-124, 2011.

[7] X. Wang, "Horizontal push load test and analysis of indoor railing of a commercial complex," *Shanxi architecture*, no. 11, pp. 36-37, 2017.

[8] F. Peng, Y. Qi, Y. Lieping et al., "Study on mechanical properties and structural safety of GFRP railings," *FRP/Composites*, no. 6, pp. 48–54, 2010.

[9] X. Cui, X. Zhang, and Z. Wu, "Research on application effect of FRP Bridge sidewalk railing engineering," *Journal of Chongqing Jianzhu University: Natural Science Edition*, vol. 35, no. 3, pp. 22–26, 2016.

[10] M. Fan, X. Liang, and J. Gao, "Study on the load effect of urban bridge railings," *Highways & Automotive Applications*, no. 3, pp. 190–193, 2014.

[11] A. Zhang and S. Guo, "Research of the overall detection method of railing thrust strength," *Municipal Engineering Technology*, no. 1, pp. 47–49, 2012.

[12] GB50009-2012, *Load Code for the Design of Building Structures*, China Architecture and Building Press, Beijing, China, 2002.

[13] CJJ69-1995, *Technical Specifications of Urban Pedestrian Overcrossing and Underpass*, The Standardization Administration of the People's Republic of China, Beijing, China, 1995.

[14] Jtg D81-2017, *Design Specifications for Highway Safety Facilities*, 2017.

[15] International Council of Building Official, *Uniform Building Code 1997*, ICC, California, LA, USA, 1997.

[16] European Committee for Standardization, *EN-1991-2. European 1 Part 2*, CEN, Brussels, Belgium, 2002.

[17] I. H. Hopkins, G. Pountney, S. J. Hayes et al., *Crowd Pressure Monitoring. Engineering for Crowd Safety*, pp. 389–398, Elsevier, Amsterdam, Netherland, 1993.

[18] R. A. Smith, "The Hillsborough football disaster: stress analysis and design codes for crush barriers," *Engineering Failure Analysis*, vol. 1, no. 3, pp. 183–192, 1994.

[19] L. Huang, D. Liu, J. Hao et al., "Experimental research on barriers design load based on body safety," *China Satefy Science Journal*, vol. 23, no. 3, pp. 22–26, 2013.

[20] China Academy of Building Research, *Technical Code for Test and Evaluation of City Bridges*, China Architecture&Building Press, Beijing, China, 2016.

[21] Y. Qi, F. Peng, and L. Ye, "Study on mechanical properties and design of railing structures," *Industrial Construction*, vol. 41, no. 5, pp. 71–79, 2011.